AIAA 81-4233

Nondestructive Buckling Test for an Integrally Stiffened Structure

Victor Weissberg*
Israel Aircraft Industries Ltd., Lod, Israel
and
Menahem Baruch†
Technion-Israel Institute of Technology, Haifa, Israel

The determination of the buckling loads on an integrally stiffened, integral wing fuel tank is described. A simplified scale test model of the relevant wing structure was built and tested under a matrix of wing bending and internal pressure loading. The local buckling load combinations were predicted using the modified Southwell-type force-stiffness method. It was confirmed that for this case the method covers the possibility of late mode changes near the buckling load better than the Southwell plot does. Hence, it was possible to obtain repeated buckling load combinations on the same specimen and thus actual buckling never occurred. At the end of this series of tests, a wing bending load was applied at zero pressure until general buckling occurred, at which point the entire test specimen failed. The problem was complicated by the fact that the wing chord was relatively large, thereby imposing plane strain and biaxial stress condition on the wing skin. The results of this work were used to construct curves of buckling stresses as functions of internal pressure for use in stress analysis and design of the wing.

Nomenclature

E	= modulus of elasticity
M	= bending moment at the center point of the column
n,m	= numbers of half waves in x and y directions
P	= longitudinal force on the column
P_{cr}	= Eulerian classical buckling load
δ	= additional lateral displacement
δ_0	= initial lateral displacement at the center of the column
ϵ_b	= bending strain at the center point of the column
ν	= Poisson ratio
σ_x, σ_y	= stress in x and y directions

Introduction

THE stress analysis of an integral fuel tank presents some problems which, in the opinion of the authors, still do not have a reliable analytical solution. These problems are as follows:

1) Appearance of local buckling under combined loading of in-plane loads and lateral loads due to pressurization.

2) Effect of local eccentricities and structural discontinuities on the local and general buckling.

3) Other unexpected phenomena peculiar to this particular structure.

It was decided to look for answers to these problems by using a static test on a representative test model. However, it was immediately realized that the usual method of testing a number of specimens to their buckling loads under different loading combinations would be prohibitively expensive because of the large size of the specimen. Consequently, a nondestructive method of testing a single specimen was sought which would predict the buckling loads under different loading combinations. The technique proposed by Donnell,[1] in the form given by Jones and Greene[2,3] with the special applications proposed here, was found to provide a reliable tool for nondestructive prediction of the general and local buckling loads of the case treated here. This is the force-stiffness (F/S) technique in which the stiffness of a given point is plotted against the load. Zero stiffness indicates the loss of stability and defines the buckling load.

It appears that the method proposed with the data obtained from the tests, processed by computer and presented in real time, may have wide industrial application for buckling predictions.

Preliminary Considerations for Performing the Tests

In the calculations of the plate buckling loads the panels between the stiffeners were assumed to be simply supported (see Fig. 1).

The theoretical envelope of buckling stresses is given by[4]

$$m^2\sigma_y + n^2\beta^2\sigma_x = \sigma_e(m^2 + n^2\beta^2)^2 \tag{1}$$

where

$$\beta = a/b$$

$$\sigma_e = \pi^2 E/12(1-\nu^2)(t/a)^2 \tag{2}$$

and m is the number of half waves in the y direction and n the number of half waves in the x direction.

This envelope formed the basis for comparison with the test results.

The factors investigated during the test were as follows: 1) internal pressure—a stabilizing factor because of the changes in the boundary conditions and the buckling mode (see Fig. 2); 2) torsional rigidity of the stiffeners—a stabilizing factor; and 3) interaction with general panel bending—bending flexibility is a destabilizing factor. An additional aim was to follow the behavior of the structure as general buckling was approached, i.e., to determine the stresses at which the buckling mode changes from one to another.

The specimen was provided with a sufficient number of strain gages (see Figs. 2-6). The loading rig is shown in Fig. 3. As is seen in this figure, it was possible to load the specimen in bending and at the same time to increase or reduce the internal pressure. In this way two of the required loads, p and N_y, may be obtained.

Received June 27, 1980; revision received Feb. 20, 1981.

*Structural Engineer.

†Professor, Department of Aeronautical Engineering. Member AIAA.

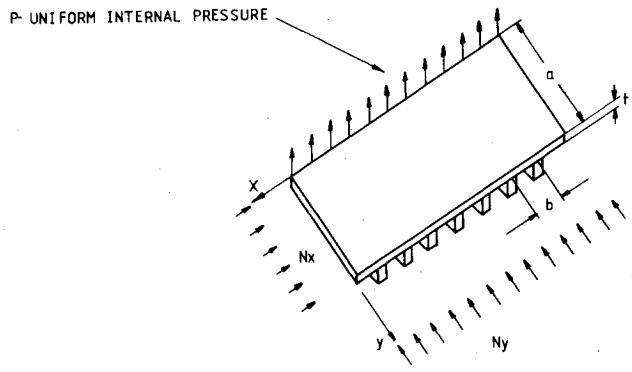

Fig. 1 Loads on integrally stiffened wing panel.

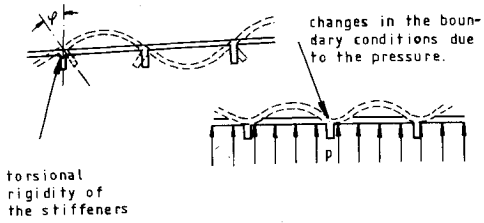

Fig. 2 Stabilizing factors.

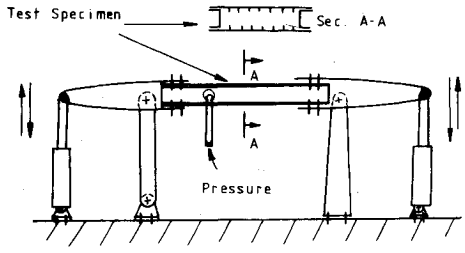

Fig. 3a Loading rig.

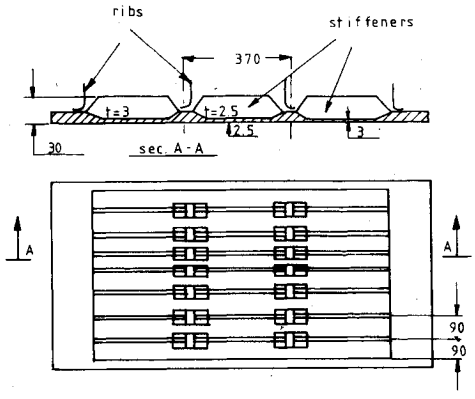

Fig. 3b Panels of test specimen.

In order to obtain the load N_x five frames were mounted around the box to restrain lateral expansion. By making the frames out of heavy steel channels, the restrained rigidities were very large compared to the lateral panel rigidities. From Hooke's law

$$\epsilon_x = (N_x - \nu N_y)/E_t \approx 0$$

$$N_x \approx \nu N_y \approx 0.33\, N_y \qquad (3)$$

where ϵ_x is the strain in the lateral direction, E the Young's modulus, and ν the Poisson ratio.

Although this method is not normally used, it gave excellent results.

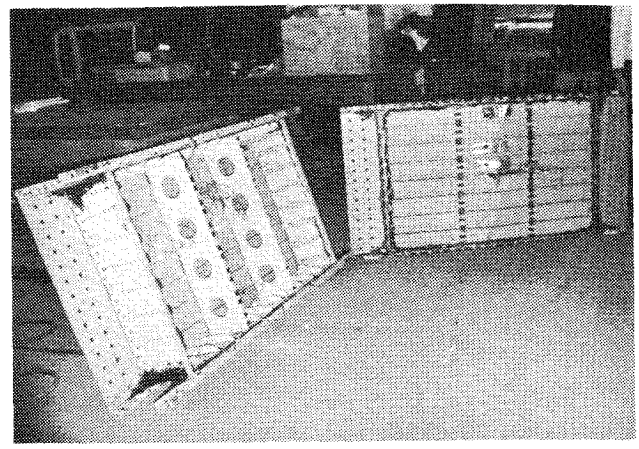

Fig. 4 Specimen before assembly.

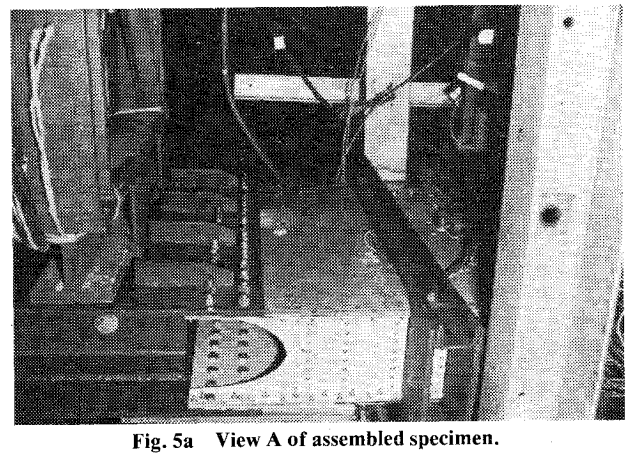

Fig. 5a View A of assembled specimen.

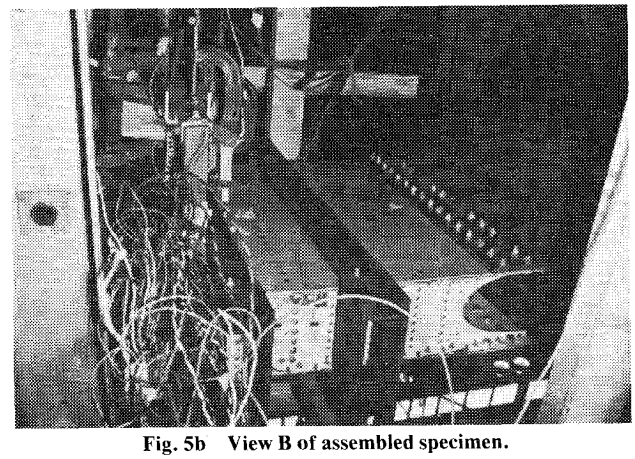

Fig. 5b View B of assembled specimen.

"Southwell" Plot: Nondestructive Prediction Techniques for Buckling

Horton et al.[5,6] gave an excellent review of the history, development, and applicability of the so-called "Southwell plot." For convenience of the reader some of their main findings will be repeated here.

It seems that Thomas Young[7] was the first to describe the hyperbolic law which connects the elastic displacement with the initial bow, the Euler critical load, and the applied axial load. Ayrton and Perry[8] gave a graphical interpretation of the hyperbolic law by which the Euler classical load can be predicted. However their work has been virtually ignored. Southwell[9] redeveloped independently a somewhat different graphical method for prediction of the buckling load. This method is the famous "Southwell plot." Finally, Donnell[1] gave a third graphical interpretation of the basic hyperbolic

law. The Donnell interpretation, which is essentially the F/S technique, was used in this work.

Many researchers have made contributions in the development of the "Southwell plot." A large list references connected with these developments can be found in Refs. 5 and 6. The main conclusion of Horton et al.[5,6] is that the "Southwell plot" is applicable not only for struts for also for plates.

The Jones and Green[2,3] version of the Donnell[1] interpretation of the hyperbolic law was found here to be the most suitable for use in a computerized graphical technique in tests with information from many strain gages. This information was used to predict the buckling load during the test in "real time." It must be noted that Jones and Green[2,3] also proposed a method in which the maximum total strain (i.e., from a single strain gage instead of the bending strain) is used in the F/S plot. In this less convenient approach, the F/S plot loses its linearity. However this plot can also be used for prediction of the buckling load. A further development of the nonlinear F/S plot can be found in Ref. 10.

Some of the considerations given by Jones and Green[2] for preferring the F/S plot over the usual Southwell plot will be repeated here for convenience of the reader.

If a simply supported beam column has a small initial lateral displacement δ_0, the deflection at the same point can be described with good accuracy by

$$\delta + \delta_0 = \frac{\delta_0}{1-(P/P_{cr})} \tag{4}$$

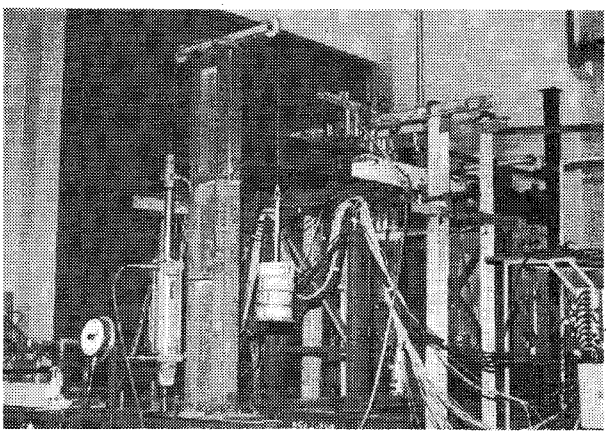

Fig. 6a General view of test rig.

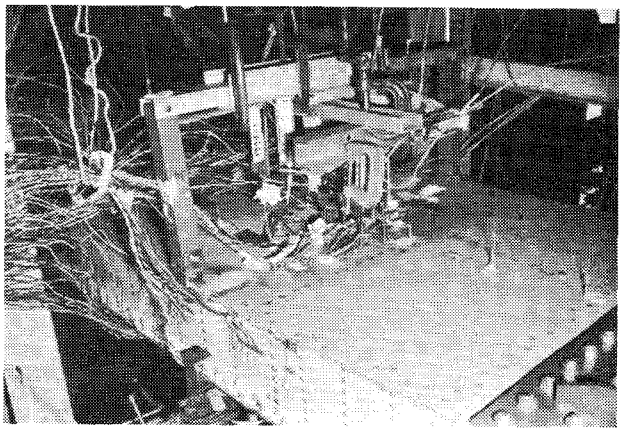

Fig. 6b General view of specimen with dial gages (DG) and strain gages (SG).

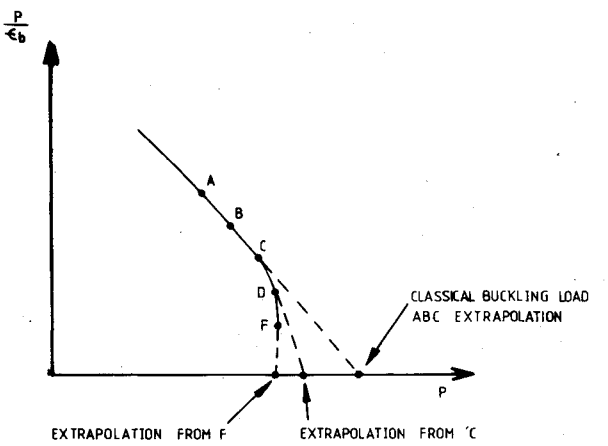

Fig. 7 F/S plot.

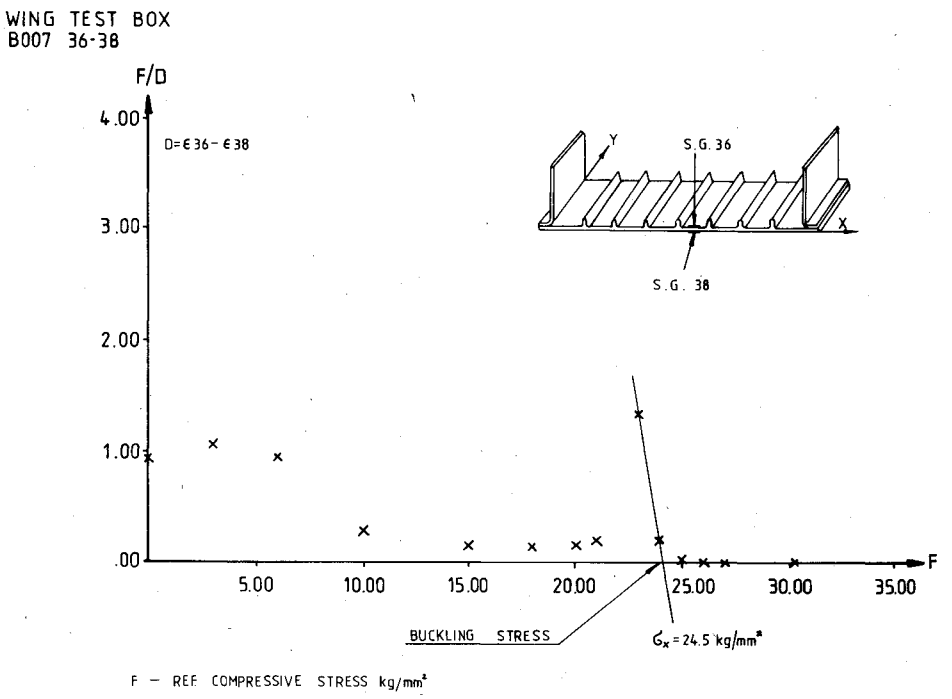

Fig. 8 F/S plot for local buckling test. Test specimen loaded only in longitudinal direction.

where P_{cr} is the Eulerian classical buckling load and δ the additional deflection.

The moment M at the center point at the column is given by

$$M=P(\delta+\delta_0) \tag{5}$$

Usually the buckling load is predicted by using strain gage data. The bending strain ϵ_b at the center of the beam column is given by

$$\epsilon_b=kM=kP(\delta+\delta_0) \tag{6}$$

where k is a constant which depends on the material and cross-sectional properties of the beam column.

Using Eq. (6), Eq. (4) can be brought to the following form

$$\frac{P}{\epsilon_b}=\frac{1}{k\delta_0}-\frac{P}{k\delta_0 P_{cr}} \tag{7}$$

Now in a plot of P/ϵ_b vs P, the classical buckling load P_{cr} will appear where the plot crosses the abscissa. The difference between the plot proposed by Donnell[1] and the one described here[2] is that the abscissa and the ordinate are interchanged. In the opinion of the authors this interchange makes the use of the Donnell plot more convenient.

In the usual Southwell plot, ϵ_b/P vs ϵ_b, the critical load is estimated from the slope of the plot. This fact makes the use of the Southwell plot less convenient than the F/S method. The F/S method is especially useful when the F/S plot due to nonlinear effects becomes nonlinear itself. In this case, it is much more difficult to calculate the slopes and therefore the application of the usual Southwell plot for estimation of the load causing failure is not convenient. When the F/S plot is used the extrapolation of the plot seems to be easier and therefore the estimation of the failure load can be calculated with more confidence.

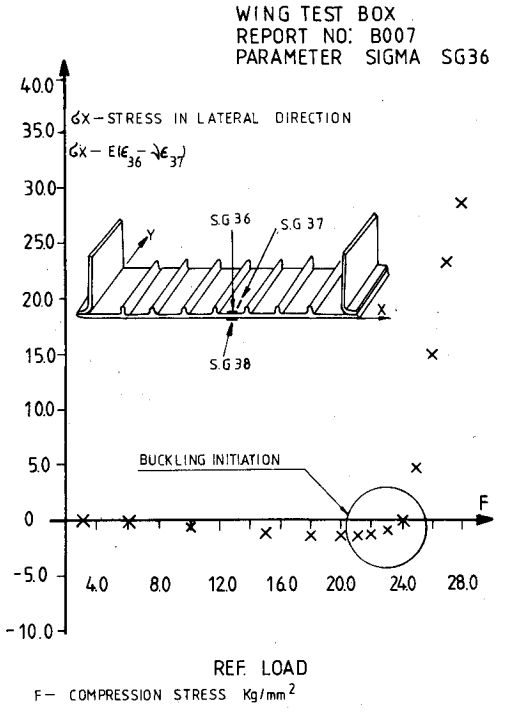

Fig. 9 Plot of stress vs longitudinal loading on plate.

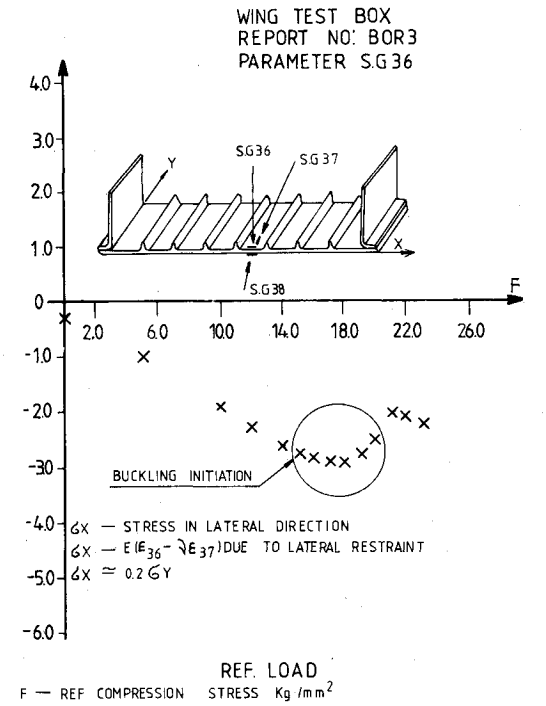

Fig. 10 Plot of lateral stress vs longitudinal loading on plate.

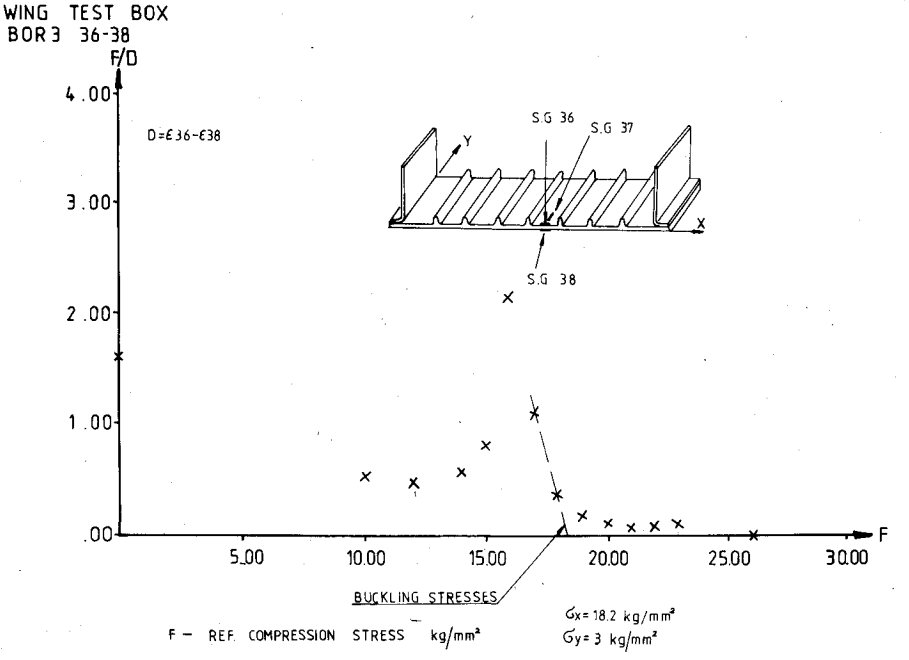

Fig. 11 F/S plot for local buckling (the test specimen was loaded with lateral restrain, $\sigma_x=0.2\sigma_y$).

To make the above considerations clearer examine Fig. 7 which is a simplified version of Fig. 3 of Ref. 2. The classical buckling load is estimated by extrapolation of the straight line ABC. If one continues to load the structure the F/S plot becomes nonlinear and the failure load can be estimated by extrapolation from point D. A better estimation of the failure load can be made by further loading of the structure and extrapolation from point F. It is clear from Fig. 7 that it is easy to computerize the F/S plot for real-time estimation of the failure load during the tests.

Application of F/S Technique in Tests for Prediction of Local Buckling

Local buckling is defined as the instability of the panels between the stiffeners. In Fig. 8 the local buckling was predicted by the F/S technique. In this test the plate was loaded longitudinally without lateral restrain ($\sigma_x = 0$).

Figure 9 shows plots of lateral stresses σ_x of the plate against the applied load. Figure 10 shows the lateral stresses σ_x against applied load. In this case the plate was restrained laterally. Figure 11 shows the prediction of buckling by F/S technique when the plate was loaded longitudinally and restrained laterally, $\sigma_x = 0.2\sigma_y$.‡

‡Figures 8-13 are copies of the graphs obtained from the computer in real time during the performance of the tests.

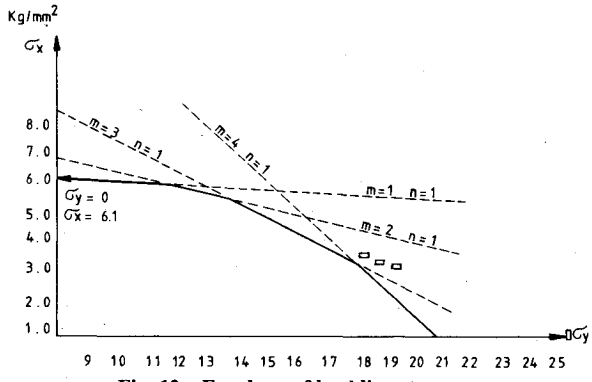

Fig. 12 Envelope of buckling stresses.

Buckling stresses obtained by the F/S technique in the tests were compared with the buckling stresses envelope obtained using Eq. (1). The results of the comparison are shown in Fig. 12.

Application of F/S Technique in Tests for Prediction of General Buckling

General buckling is defined as the instability of the panels with the stiffeners behaving as a beam column. Figure 13 shows the prediction of the general buckling by the F/S technique. Results of F/S extrapolation show that the structure will buckle in a general mode at a reference compression stress of 31.7 kg/mm^2. The F/S plot also shows that there is a change in the buckling mode at the reference stress of 20 kg/mm^2.

After the completion of the combined bending and pressure tests, the test specimen was loaded until the general buckling was reached. The structure buckled at a reference stress of 30 kg/mm^2. It was found that the small difference between the predicted F/S buckling stress and the destruction test results must have been due to an imperfection in the flanges of the test specimen (see Fig. 14).

In Ref. 10, where tests were performed on a similar structure (a wing of the Mirage 2000), Finance comes to the conclusion that in modern stiff wing structures the load of failure of the structure is usually somehow less than that predicted by the F/S plot buckling load. The explanation is that for loads close to the load of failure there are local moments which together with stresses deep in the plastic region cause a fast growing of deformation and failure. However, in the case treated here the difference between the predicted buckling stress (31.7 kg/mm^2) and the stress of failure obtained during the test (30 kg/mm^2) was acceptably small.

It is interesting to compare the destruction buckling test stress with that obtained from a finite-element NASTRAN program (which uses the differential stiffness technique).[11] The results of the finite-element analysis gives the first three buckling mode shapes and the corresponding stresses (see Fig. 15).

In the destruction test it was observed that the structure tends initially to buckle in the third mode shape, which corresponds to a critical compressive stress of about 100 kg/mm^2. This mode is clearly enforced by the initial ec-

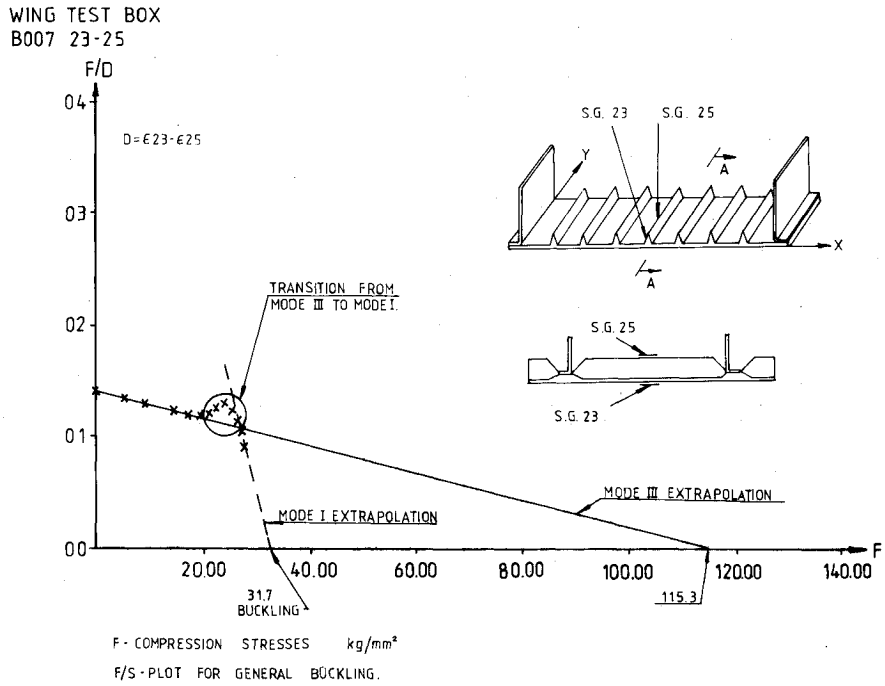

Fig. 13 F/S plot for general buckling.

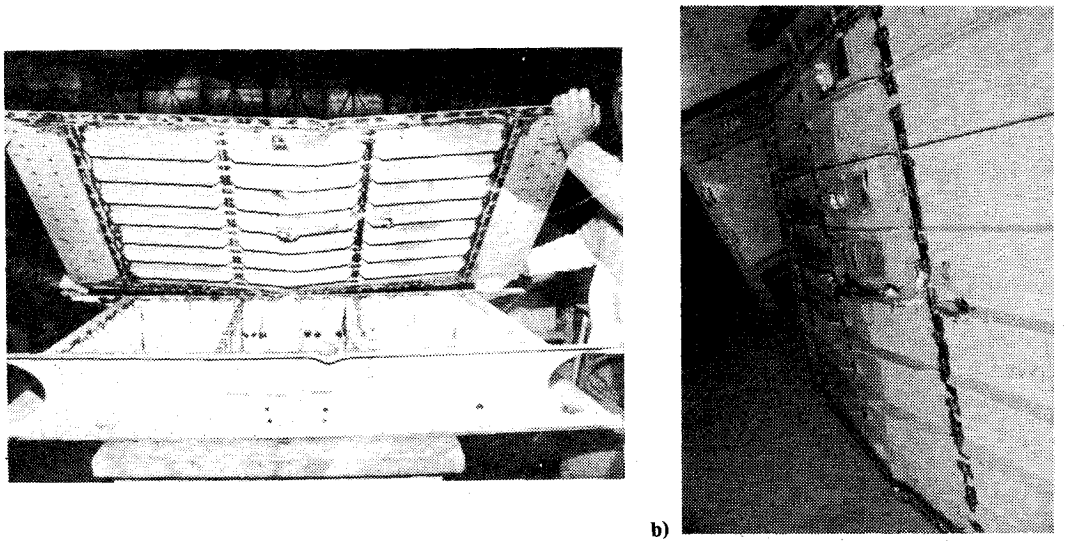

Fig. 14 a) View A of buckled specimen. b) View B of buckled specimen.

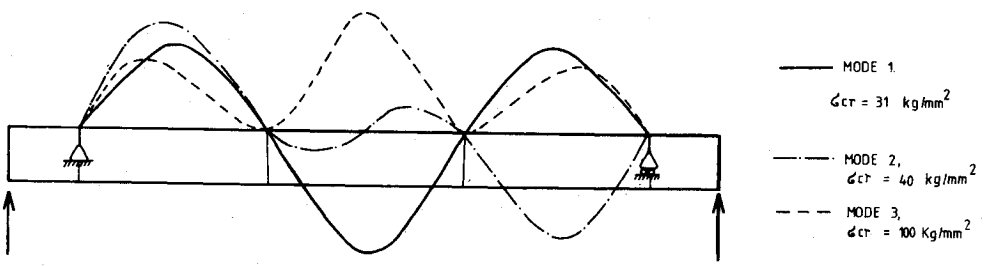

	MODE 3	MODE 2	MODE 1
NASTRAN	100 kg/mm²	40,3 Kg/mm²	31 Kg/mm²
TEST WITH F/S INTERPRETATION	115 Kg/mm²		31,7 Kg/mm²
TRANSITION STRESS	20 Kg/mm² FROM MODE 3 TO MODE 1		

Fig. 15 Result of finite-element analysis for general buckling.

centricities. At a stress of 20 kg/mm² the mode changes from the third to the first, which corresponds to a critical compressive stress of 31.7 kg/mm².

The second mode (critical compressive stress of approximately 40 kg/mm²) was not observed, probably because it is nonsymmetric and the loading, the structure, and boundary condition are symmetrical toward the same axis.

Conclusions

The results from the completed test provided the factors listed in the Introduction to this paper:

1) The applied internal pressure of up to 15 psi provided no significant stabilization to the panels.

2) The torsional rigidity of the stiffeners increase the buckling allowables by about 15% as compared to the allowables for the simply supported condition.

3) Although the local buckling stress (25 kg/mm²) was close to the general buckling stress (30 kg/mm²), there was no evidence of local influence on the general buckling stress or vice versa.

4) Prediction of buckling load by the F/S technique was found to be very useful and easy to handle.

References

[1] Donnell, L.H., "On the Application of Southwell's Method for Analysis of Buckling Tests," *Stephen Timoshenko 60th Anniversary Volume*, McGraw Hill Book Co., 1938, pp. 27-38.

[2] Jones, R.E. and Green, B.E., "Force/Stiffness Technique for Nondestructive Buckling Testing," *Journal of Aircraft*, Vol. 13, April 1976, pp. 262-269.

[3] Musgrove, M.D., Green, B.E., Shideler, J.L., and Bohon, H.L., "Advanced Beaded and Tabular Structural Panels," *Journal of Aircraft*, Vol. 11, Feb. 1974, pp. 68-75.

[4] Timoshenko, S.P. and Gere, I.M., *Theory of Elastic Stability*, 2nd Ed., McGraw Hill Book Co., New York, 1961.

[5] Horton, W.H., Cundari, F.L., and Johnson, R.W., "A Review of the Applicability of the 'Southwell' Plot to the Interpretation of Test Data Obtained from Stability Studies of Elastic Column and Plate Structures," Dept. of Aeronautics and Astronautics, Stanford University, Stanford, Calif., SUDAAR 296, Dec. 1966.

[6] Horton, W.H., Cundari, F.L., and Johnson, R.W., "The Analysis of Experimental Data Obtained from Stability Studies on Elastic Column and Plate Structures," *Israel Journal of Technology*, Vol. 5, Nos. 1-2, 1967, pp. 104-113.

[7] Young, T., *A Course of Lectures on Natural Philosophy and the Mechanical Arts*, 1st Ed., Vol. 11, Sec. IX, London, 1807, p. 47.

[8] Ayrton, W.E., Perry, J., "On Struts," *The Engineer*, Vol. 62, 1886, pp. 464-465 and 513-515.

[9] Southwell, R.V., "On the Analysis of Experimental Observations in Problems of Elastic Stability," *Proceedings of the Royal Society* (London), Series A, Vol. 135, 1932, pp. 601-616.

[10] Finance, I.P.A., "Methodes Experimentales Contribuatant a la Prevision des Ruptures lors des Assais de Resistance sur Structures Complexes," *L'Aeronautique et L'Astronautique*, No. 78, 1979, pp. 67-74.

[11] "MSC/NASTRAN Theoretical Manual," Macneal Schwendler Corp., May 1976.